International Journal of Engineering and Applied Sciences (IJEAS)
Vol.1, Issue 3(2009)1-11

STATIC ANALYSIS OF A FUNCTIONALLY GRADED BEAM UNDER A UNIFORMLY DISTRIBUTED LOAD BY RITZ METHOD

M. Şimşek
Yıldız Technical University, Department of Civil Engineering, Davutpaşa Campus, 34210 Esenler-İstanbul, Turkey

Accepted Date: 09 June 2009

Abstract

Static analysis of a functionally graded (FG) simply-supported beam subjected to a uniformly distributed load has been investigated by using Ritz method within the framework of Timoshenko and the higher order shear deformation beam theories. The material properties of the beam vary continuously in the thickness direction according to the power-law form. Trial functions denoting the transverse, the axial deflections and the rotation of the cross-sections of the beam are expressed in trigonometric functions. In this study, the effect of various material distributions on the displacements and the stresses of the beam are examined. Numerical results indicate that stress distributions in FG beams are very different from those in isotropic beams.

Keywords: Beams, functionally graded materials, Timoshenko beam theory, the higher order shear deformation theory, Ritz method.

1. Introduction

In material sciences, a functionally graded material (FGM) is a type of material whose composition is designed to change continuously within the solid. The concept is to make a composite material by varying the microstructure from one material to another material with a specific gradient. This enables the material to have good specifications of both materials. If it is for thermal or corrosive resistance or malleability and toughness, both strengths of the material may be used to avoid corrosion, fatigue, fracture and stress corrosion cracking. The transition between the two materials can usually be approximated by means of a power series. The aircraft and aerospace industry and the computer circuit industry are very interested in the possibility of materials that can withstand very high thermal gradients. This is normally achieved by using a ceramic layer connected with a metallic layer. The concept of FGM was first considered in Japan in 1984 during a space plane project. The FGM materials can be designed for specific applications. For example, thermal barrier coatings for turbine blades (electricity production), armor protection for military applications, fusion energy devices, biomedical materials including bone and dental implants, space/aerospace industries, automotive applications, etc.

Static and dynamic analyses of FGM structures have attracted increasing research effort in the last decade because of the wide application areas of FGMs. For instance, Sankar [1] gave an elasticity solution based on the Euler-Bernoulli beam theory for functionally graded beam subjected to static transverse loads by assuming that Young's modulus of the beam vary exponentially through the thickness. Chakraborty et al. [2] proposed a new beam finite element based on the first-order shear deformation theory to study the thermoelastic behavior

of functionally graded beam structures. In [2], static, free and wave propagation analysis are carried out to examine the behavioral difference of functionally graded material beam with pure metal or pure ceramic. Chakraborty and Gopalakrishnan [3] analyzed the wave propagation behavior of FG beam under high frequency impulse loading, which can be thermal or mechanical, by using the spectral finite element method. Aydogdu and Taskin [4] investigated the free vibration behavior of a simply supported FG beam by using Euler-Bernoulli beam theory, parabolic shear deformation theory and exponential shear deformation theory. Zhong and Yu [5] presented an analytical solution of a cantilever FG beam with arbitrary graded variations of material property distribution based on two-dimensional elasticity theory. Ying et al. [6] obtained the exact solutions for bending and free vibration of FG beams resting on a Winkler-Pasternak elastic foundation based on the two- dimensional elasticity theory by assuming that the beam is orthotropic at any point and the material properties vary exponentially along the thickness direction. Kapuria et al. [7] presented a finite element model for static and free vibration responses of layered FG beams using an efficient third order zigzag theory for estimating the effective modulus of elasticity, and its experimental validation for two different FGM systems under various boundary conditions. Yang and Chen [8] studied the free vibration and elastic buckling of FG beams with open edge cracks by using Euler-Bernoulli beam theory. Li [9] proposed a new unified approach to investigate the static and the free vibration behavior of Euler-Bernoulli and Timoshenko beams. In a recent study by Yang et al. [10], free and forced vibrations of cracked FG beams subjected to an axial force and a moving load were investigated by using the modal expansion technique. Kadoli et al. [11] studied the static behavior of a FG beam by using higher order shear deformation theory and finite element method. Benatta et al. [12] proposed an analytical solution to the bending problem of a symmetric FG beam by including warping of the cross-section and shear deformation effect. Sallai et al. [13] investigated the static responses of a sigmoid FG thick beam by using different beam theories. Sina et al. [14] used a new beam theory different from the traditional first-order shear deformation beam theory to analyze the free vibration of a FG beams. Şimşek and Kocatürk [15] have recently investigated the free and forced vibration characteristics of a FG Euler-Bernoulli beam under a moving harmonic load. Şimşek [16] studied the dynamic deflections and the stresses of an FG simply-supported beam subjected to a moving mass by using Euler-Bernoulli, Timoshenko and the higher order shear deformation theories by considering the centripetal, inertia and Coriolis effects of the moving mass.

As it is known, Timoshenko beam theory (TBT) or the first order shear deformation theory in which straight lines perpendicular to the mid-plane before bending remain straight, but no longer remain perpendicular to the mid-plane after bending. In TBT, the distribution of the transverse shear stress with respect to the thickness coordinate is assumed constant. Thus, a shear correction factor is required to compensate for the error because of this assumption in TBT. However, studies in the literature show that TBT gives satisfactory results and it is very effective to investigate behavior of beams and plates. The higher order shear deformation theory (HOSDT) or the third order shear deformation theory which assumed parabolic distribution of the transverse shear stress and strain with respect to the thickness coordinate was proposed for beams with rectangular cross-sections by Reddy [17]. Consequently, zero transverse shear stress condition of the upper and lower fibers of the cross-section is satisfied without a shear correction factor in HOSDT.

The aim of this paper is to investigate the static analysis of a functionally graded simply-supported beam under a uniformly distributed load by Ritz method. It is assumed that material properties of the beam vary continuously in the thickness direction according to the power-

law. In this study, various material distributions on the displacements and the stresses of the FG beam are examined.

2. Theory and Formulations

A functionally graded simply-supported beam of length *L*, width *b*, thickness *h*, with co-ordinate system $(\mathrm{O}\,x\,y\,z)$ having the origin O is shown in Fig.1. The beam is subjected to a uniformly distributed load, q.

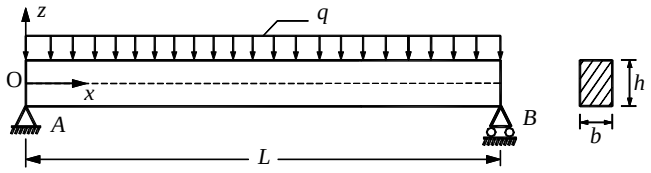

Fig. 1. A functionally graded simply-supported beam subjected to a uniformly distributed load.

In this study, it is assumed that the FG beam is made of ceramic and metal, and the effective material properties of the FG beam, i.e., Young's modulus E, Poisson's ratio υ and shear modulus G vary continuously in the thickness direction (z axis direction) according to power-law form introduced by [18]

$$E(z)=(E_m-E_c)\left(\frac{z}{h}+\frac{1}{2}\right)^k+E_c \tag{1}$$

$$\upsilon(z)=(\upsilon_m-\upsilon_c)\left(\frac{z}{h}+\frac{1}{2}\right)^k+\upsilon_c \tag{2}$$

$$G(z)=\frac{E(z)}{2(1+\upsilon(z))} \tag{3}$$

where k is the non-negative variable parameter (power-law exponent) which dictates the material variation profile through the thickness of the beam, m and c stand for metal and ceramic constituents, respectively.

It is clear from Eqs. (1-3) that

$$E=E_c,\ \ \upsilon=\upsilon_c,\ \ G=G_c \ \text{ at } \ z=-h/2 \tag{4a}$$

$$E=E_m,\ \ \upsilon=\upsilon_m,\ \ G=G_m \ \text{ at } \ z=h/2 \tag{4b}$$

Fig. 2 shows variation of the modulus of elasticity through the thickness of the beam.

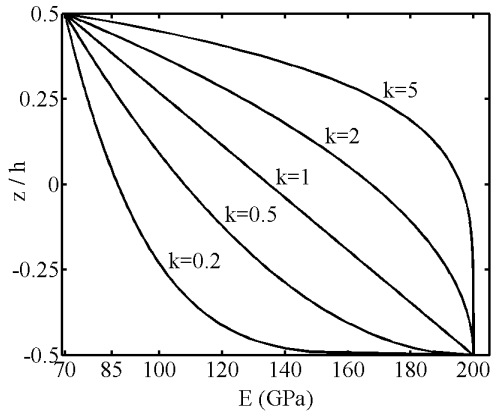

Fig. 2. Variation of the modulus of elasticity through the thickness of the FG beam.

Based on the higher order shear deformation theory, the axial displacement, u_x, and the transverse displacement of any point of the beam, u_z, are given as [17]

$$u_x(x,z) = u_0(x) + z\phi(x) - \alpha z^3\left(w_{0,x}(x) + \phi(x)\right) \tag{5a}$$

$$u_z(x,z) = w_0(x) \tag{5b}$$

where u_0 and w_0 are the axial and the transverse displacement of any point on the neutral axis, ϕ is the rotation of the cross-sections, $\alpha = 4/(3h^2)$, and $(\,)_{,x}$ indicates the derivative with respect to x. The strain-displacement relations are given by

$$\varepsilon_{xx} = u_{x,x} = u_{0,x} + z\phi_{,x} - \alpha z^3\left(\phi_{,x} + w_{0,xx}\right) \tag{6a}$$

$$\gamma_{xz} = u_{x,z} + u_{z,x} = \left(1 - 3\alpha z^2\right)\left(\phi + w_{0,x}\right) \tag{6b}$$

where ε_{xx} and γ_{xz} are the normal and the shear strain, respectively. By assuming that the material of FGM beam obeys Hooke's law, the stresses in the beam become

$$\sigma_{xx} = E(z)\,\varepsilon_{xx} \tag{7a}$$

$$\tau_{xz} = G(z)\,\gamma_{xz} \tag{7b}$$

where σ_{xx} and γ_{xz} are the axial normal and the shear stresses. The strain energy of the beam at any instant in Cartesian coordinates is given as

$$U_i = \frac{1}{2}\int_0^L \int_A \left(\sigma_{xx}\,\varepsilon_{xx} + \tau_{xz}\,\gamma_{xz}\right) \mathrm{d}A\,\mathrm{d}x \tag{8}$$

where A is the area of the cross-section of the beam. Substituting Eqs. (6, 7) into Eq. (8) leads to

$$U_i = \frac{1}{2}\int_0^L \Big\{ A_{xx}\left(u_{0,x}\right)^2 + 2\left(B_{xx} - \alpha E_{xx}\right)\left(u_{0,x}\right)\left(\phi_{,x}\right) - 2\alpha E_{xx}\left(u_{0,x}\right)\left(w_{0,xx}\right)$$
$$+\left(D_{xx} + \alpha^2 H_{xx} - 2\alpha F_{xx}\right)\left(\phi_{,x}\right)^2 + 2\alpha\left(\alpha H_{xx} - F_{xx}\right)\left(w_{0,xx}\right)\left(\phi_{,x}\right) + \alpha^2 H_{xx}\left(w_{0,xx}\right)^2$$
$$+\left(A_{xz} - 6\alpha D_{xz} + 9\alpha^2 F_{xz}\right)\left[\left(\phi^2\right) + 2\left(\phi\right)\left(w_{0,x}\right) + \left(w_{0,x}\right)^2\right]\Big\}\,\mathrm{d}x \tag{9}$$

where

$$\left(A_{xx}, B_{xx}, D_{xx}, E_{xx}, F_{xx}, H_{xx}\right) = \int_A E(z)\left(1,\ z,\ z^2,\ z^3,\ z^4,\ z^6\right)\mathrm{d}A \tag{10a}$$

$$\left(A_{xz},\ D_{xz},\ F_{xz}\right) = \int_A G(z)\left(1,\ z^2,\ z^4\right)\mathrm{d}A \tag{10b}$$

Potential of the uniformly distributed load is given below

$$U_e = -\int_0^L q(x)\, w_0(x)\,\mathrm{d}x \tag{11}$$

Therefore, the total potential energy of the problem can be written as

$$\Pi = U_i + U_d \tag{12}$$

The boundary conditions of the simply-supported beam are given by

$$u_0(x) = 0 \text{ at } x = 0, \quad w_0(x) = 0 \text{ at } x = 0,\ L \tag{13}$$

As it is known, when some expressions satisfying kinematic boundary conditions are selected for $w_0(x)$, $u_0(x)$ and $\phi(x)$ then by using the principle of the minimum potential energy, the natural (dynamic) boundary conditions are also satisfied. The displacements $w_0(x)$, $u_0(x)$ and rotation $\phi(x)$ are expanded by the following series which satisfy the kinematic boundary conditions in Eq. (13);

$$w_0(x) = \sum_{n=1}^{N} A_n\, \theta_n(x) \tag{14a}$$

$$u_0(x) = \sum_{n=1}^{N} B_n\, \psi_n(x) \tag{14b}$$

$$\phi(x) = \sum_{n=1}^{N} C_n\, \varphi_n(x) \tag{14c}$$

where A_n, B_n and C_n are the unknown coefficients to be determined, $\theta_n(x)$, $\psi_n(x)$ and $\varphi_n(x)$ are the space-dependent functions (admissible functions) which are chosen in this study from the trigonometric functions, and given as follows:

$$\theta_n(x) = \sin\frac{n\pi x}{L}, \tag{15a}$$

$$\psi_n(x) = \sin\frac{(2n-1)\pi x}{2L} \tag{15b}$$

$$\varphi_n(x) = \cos\frac{n\pi x}{L}, \tag{15a}$$

By introducing the following definitions,

$$q_n = A_n \qquad n = 1, 2, ..., N \tag{16a}$$

$$q_n = B_{n-N} \qquad n = N+1, ..., 2N \tag{16b}$$

$$q_n = C_{n-2N} \qquad n = 2N+1, ..., 3N \tag{16c}$$

and after substituting Eqs.(14a, b, c) into Eq. (12) and then using the principle of the minimum potential energy given by Eq. (17)

$$\frac{\partial \Pi}{\partial q_n} = 0 \qquad n = 1, 2, ..., 3N \tag{17}$$

yields the following system of equations

$$\begin{bmatrix} [\mathrm{K}_1]_{N\times N} & [\mathrm{K}_2]_{N\times N} & [\mathrm{K}_3]_{N\times N} \\ [\mathrm{K}_4]_{N\times N} & [\mathrm{K}_5]_{N\times N} & [\mathrm{K}_6]_{N\times N} \\ [\mathrm{K}_7]_{N\times N} & [\mathrm{K}_8]_{N\times N} & [\mathrm{K}_9]_{N\times N} \end{bmatrix} \begin{Bmatrix} \mathrm{A} \\ \mathrm{B} \\ \mathrm{C} \end{Bmatrix} = \begin{Bmatrix} \mathrm{f} \\ 0 \\ 0 \end{Bmatrix} \tag{18}$$

where $[\mathrm{K}_1], ..., [\mathrm{K}_9]$ are the stiffness matrices of the beam, f is the generalized load vector generated by the uniformly distributed load. It is also note that TBT is a special case of HOSDT and the equations of equilibrium for TBT are obtained by taking $\alpha = 0$ and $\bar{A}_{xz} = k_s A_{xz}$ in Eq. (18).

3. Numerical Results

In numerical results, the static responses of an FG simply-supported beam are investigated. Functionally graded material (FGM) of the beam is composed of Aluminum (Al; $E_m = 70$ GPa, ν_m=0.3) and Zirconia ($\mathrm{ZrO_2}$; $E_c = 200$ GPa, ν_c=0.3) and its properties changes through the thickness of the beam according to the power-law. The bottom surface of the FG beam is pure Zirconia, whereas the top surface of the beam is pure Aluminum. The width and the thickness of the beam are kept constant as $b = 0.1$ m and $h = 0.1$ m, respectively. The length of the beam is taken as $L = 0.3$ m, $L = 0.4$ m and L =1.6 m for three different values of slenderness ratio, $L/h = 3, 4, 16$. The shear correction factor is considered as $k_s = 5/6$ for TBT. The axial and the transverse displacements of the beam are normalized by the static deflection, $w_{\text{static}} = 5qL^4 / 384 E_{\text{Al}} I$, of the fully aluminum beam

under the uniformly distributed load. The axial normal stresses, σ_{xx}, are calculated at the midpoint of the beam ($x = L/2$), and the shear stresses, τ_{xz}, are evaluated at the left support of the beam ($x = 0$), and the normal and the shear stresses are normalized by $(\bar{\sigma}_{xx}, \bar{\tau}_{xz}) = \left(\frac{\sigma_{xx} A}{qL}, \frac{\tau_{xz} A}{qL} \right)$. In this study, the compressive and the tensile normal stresses are represented by positive and negative signs, respectively. Also, it is seen that the numerical accuracy of the responses is satisfactory when the number of terms in the displacement functions is set to $N = 14$.

In Table 1, maximum non-dimensional deflections of the beam are presented for various values of power-law exponent and for $L/h = 4, 16$. It is seen from Table 1 that as the value of the power-law exponent increases, the deflections of the beam decrease. This is due to the fact that an increase in the power-law exponent yields a decrease in the bending rigidity of the beam, as also seen by inspecting Fig. 2. As would be expected, the deflection of the full aluminum beam is maximum whereas it is minimum for the full Zirconia beam. Note also that the deflections of TBT and HOSDT are very close to each other. As is known, shear deformation effect plays an important role on the responses of the short beams, and the displacements of the shear deformable beam theories are larger than those of Euler-Bernoulli beam theory. This effect is clearly seen for full metal beam with $L/h = 4$.

Table 1. Maximum non-dimensional transverse deflection of the beam for various values of power-law exponent

Power-law exponent	Theory	Maximum non-dimensional transverse deflection	
		$L/h = 4$	$L/h = 16$
$k = 0$ (Full metal)	TBT	1.13002	1.00812
	HOSDT	1.15578	1.00975
$k = 0.2$	TBT	0.84906	0.75595
	HOSDT	0.87145	0.75737
$k = 0.5$	TBT	0.71482	0.63953
	HOSDT	0.73264	0.64065
$k = 1$	TBT	0.62936	0.56615
	HOSDT	0.64271	0.56699
$k = 2$	TBT	0.56165	0.50718
	HOSDT	0.57142	0.50780
$k = 5$	TBT	0.49176	0.44391
	HOSDT	0.49978	0.44442
Full ceramic	TBT	0.39550	0.35284
	HOSDT	0.40452	0.35341

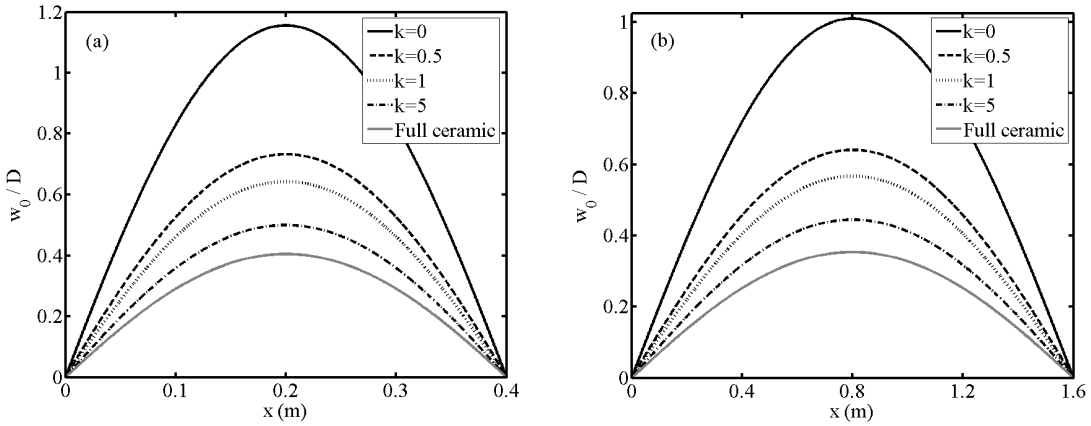

Fig.3. Non-dimensional transverse displacements along the length of the beam for a) $L/h=4$ b) $L/h=16$.

Figs. 3 and 4 show the non-dimensional transverse and the axial displacements along the length of the beam, respectively. As stated before, when the power-law exponent is increased, the displacements of the FG beam are decreased. The axial displacements of the full metal and full ceramic beams are zero and coincide with each other. Because, in full metal and the full ceramic beams (isotropic beams), there is no coupling between the bending and the stretching, namely $B_{xx}=E_{xx}=0$. In contrast to transverse displacements, as seen from Fig. 4, firstly, the axial displacements increase with the increase in the power-law exponent, and then decrease with further increase in the power-law exponent. It is also to be noted that as the power-law exponent increases, the composition of the FG beam approaches to the composition of the full ceramic beam.

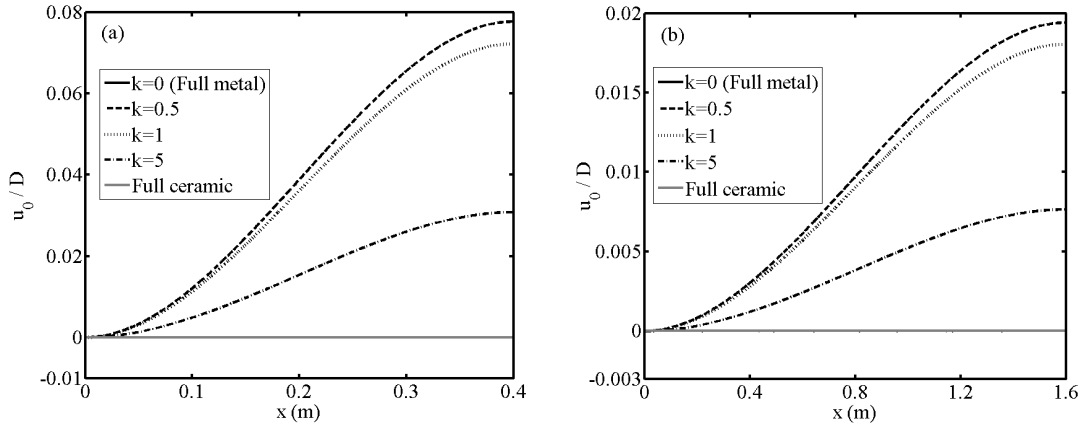

Fig. 4. Non-dimensional axial displacements along the length of the beam for a) $L/h=4$ b) $L/h=16$.

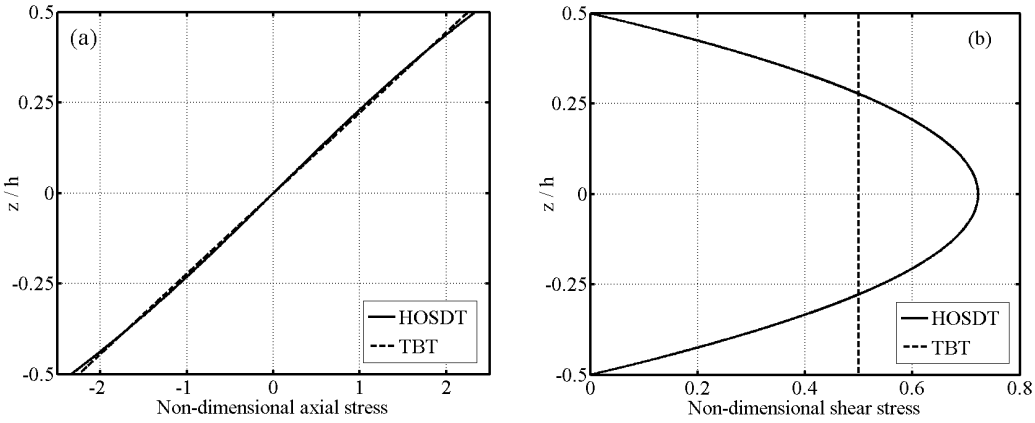

Fig. 5. Non-dimensional axial and shear stress distributions of the metal beam for $L/h=3$.

Fig. 5 displays the non-dimensional axial and the shear stress distributions of the full metal beam along the thickness of the beam. As seen from Fig. 5a, the normal stress distribution is not linear for HOSDT represented by black solid line. Also, the magnitude of the axial stresses of HOSDT is a little larger than those of TBT. The shear stress distribution is parabolic and the zero stress condition on the upper and the lower side of the cross-section is satisfied for HOSDT. Furthermore, the constant shear stress assumption of TBT is clearly seen from Fig. 5b.

Fig. 6 shows the non-dimensional axial normal stress distributions of HOSDT for various values of power-law exponent. The most significant aspect of this figure is that the axial normal stress distributions of FG beams are much more different from those in isotropic beams. Although the magnitude of the axial compressive and the axial tensile stresses have the same magnitude in full metal and full ceramic beams (isotropic beams), the magnitude of the tensile stresses are greater than the magnitude of the compressive stresses in FG beams. The value of the axial stresses is not zero at the mid-plane of the FG beam. This indicates that the neutral plane of the beam moves towards the lower side of the beam for the FG beam. This is due to the variation of the modulus of elasticity through the thickness of the FG beam.

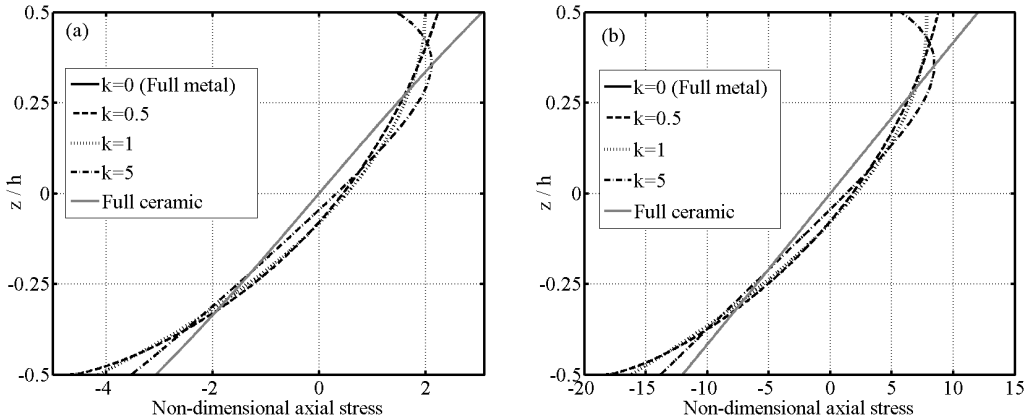

Fig. 6. Non-dimensional axial stress distributions for various values of power-law exponent, a) $L/h=4$ b) $L/h=16$.

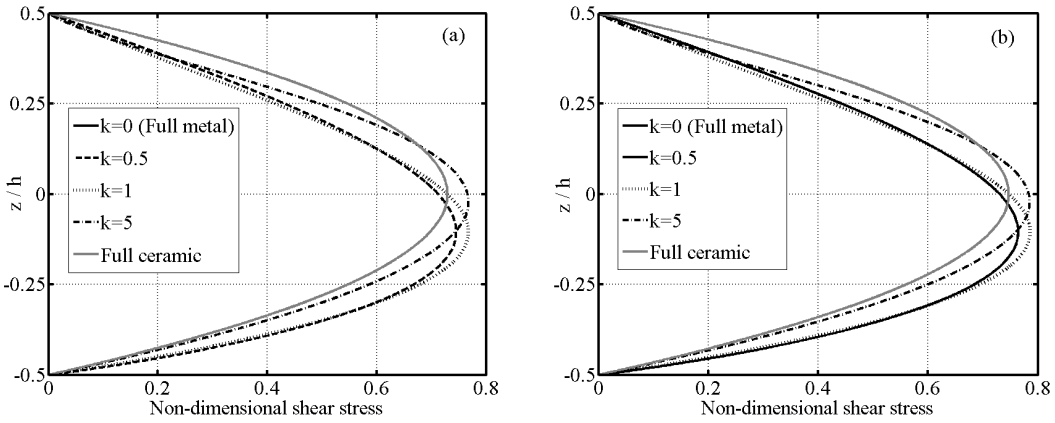

Fig. 7. Non-dimensional shear stress distributions for various values of power-law exponent, a) $L/h=4$ b) $L/h=16$.

Fig. 7 shows the non-dimensional shear stress distributions along the thickness for various values of power-law exponent. The shear stresses of the full metal and the full ceramic beam coincide with each other, and they are symmetric about the mid-plane of the beam. Also, as is known from strength of materials, it can be observed from this figure that the value of the shear stresses is maximum on the neutral axis of the beam. The shear stress distributions are greatly influenced by the power-law exponent.

4. Conclusions

Static analysis of an FG simply-supported beam subjected to a uniformly distributed load is investigated within the framework of HOSDT and TBT by using Ritz Method. Trial functions denoting the transverse, the axial deflections and the rotation of the cross-sections of the beam are expressed in trigonometric functions. The material properties of the beam vary continuously in the thickness direction according to the power-law form. Numerical results show that the variation of the modulus of elasticity plays a major role on the stress distributions and the displacements of the FG beam. Also, in the design of structures, by choosing a suitable power-law exponent, the material properties of the FG beam can be tailored to meet the desired goals of minimizing stresses and displacements in a beam-type structure.

References

[1] Sankar B.V., An elasticity solution for functionally graded beams. *Composites Sciences and Technology*, 61(5), 689-696, 2001.
[2] Chakraborty A., Gopalakrishnan S, Reddy J.N., A new beam finite element for the analysis of functionally graded materials. *International Journal of Mechanical Sciences*, 45(3), 519-539, 2003.
[3] Chakraborty A., Gopalakrishnan S., A spectrally formulated finite element for wave propagation analysis in functionally graded beams. *International Journal of Solids and Structures*, 40(10), 2421-2448, 2003.
[4] Aydogdu M., Taskin V., Free vibration analysis of functionally graded beams with simply supported edges. *Materials & Design*, 28(5), 1651-1656, 2007.

[5] Zhong Z., Yu T., Analytical solution of a cantilever functionally graded beam. *Composites Sciences and Technology*, 67(3-4), 481-488, 2007.
[6] Ying J., Lü C.F., Chen W.Q., Two-dimensional elasticity solutions for functionally graded beams resting on elastic foundations. *Composite Structures*, 84(3), 209-219, 2008.
[7] Kapuria S., Bhattacharyya M., Kumar A.N., Bending and free vibration response of layered functionally graded beams: A theoretical model and its experimental validation. *Composite Structures*, 82(3), 390-402, 2008.
[8] Yang J., Chen Y., Free vibration and buckling analyses of functionally graded beams with edge cracks. *Composite Structures*, 83(1), 48-60, 2008.
[9] Li X.F., A unified approach for analyzing static and dynamic behaviors of functionally graded Timoshenko and Euler-Bernoulli beams. *Journal of Sound and Vibration*, 318(4-5), 1210-1229, 2008.
[10] Yang J., Chen Y., Xiang Y., Jia X.L., Free and forced vibration of cracked inhomogeneous beams under an axial force and a moving load. *Journal of Sound Vibration*, 312(1-2), 166-181, 2008.
[11] Kadoli R., Akhtar K., Ganesan N., Static analysis of functionally graded beams using higher order shear deformation theory. *Applied Mathematical Modelling*, 32(12), 2509-2525, 2008.
[12] Benatta M.A., Mechab I., Tounsi A., Adda Bedia E.A., Static analysis of functionally graded short beams including warping and shear deformation effects. *Computational Materials Science*, 44(2), 765-773, 2008.
[13] Sallai B.O., Tounsi A., Mechab I., Bachir B.M., Meradjah M., Adda B.E.A., A theoretical analysis of flexional bending of Al/Al_2O_3 S-FGM thick beams. *Computational Materials Science*, 44(4), 1344-1350, 2009.
[14] Sina S.A., Navazi H.M., Haddadpour H., An analytical method for free vibration analysis of functionally graded beams. *Materials and Design*, 30(3), 741-747, 2009.
[15] Şimşek M., Kocatürk T., Free and forced vibration of a functionally graded beam subjected to a concentrated moving harmonic load. *Composite Structures*, doi:10.1016/j.compstruct.2009.04.24, 2009.
[16] Şimşek M., Vibration analysis of a functionally graded beam under a moving mass by using different beam theories, *Composite Structures*, submitted.
[17] Reddy J.N, *Energy and Variational Methods in Applied Mechanics*, John Wiley New York, 1984.
[18] Wakashima K., Hirano T., Niino M., Space applications of advanced structural materials, SP, 303-397, ESA 1990.